Published OnlineFirst March 3, 2014; DOI: 10.1158/0008-5472.CAN-13-1703

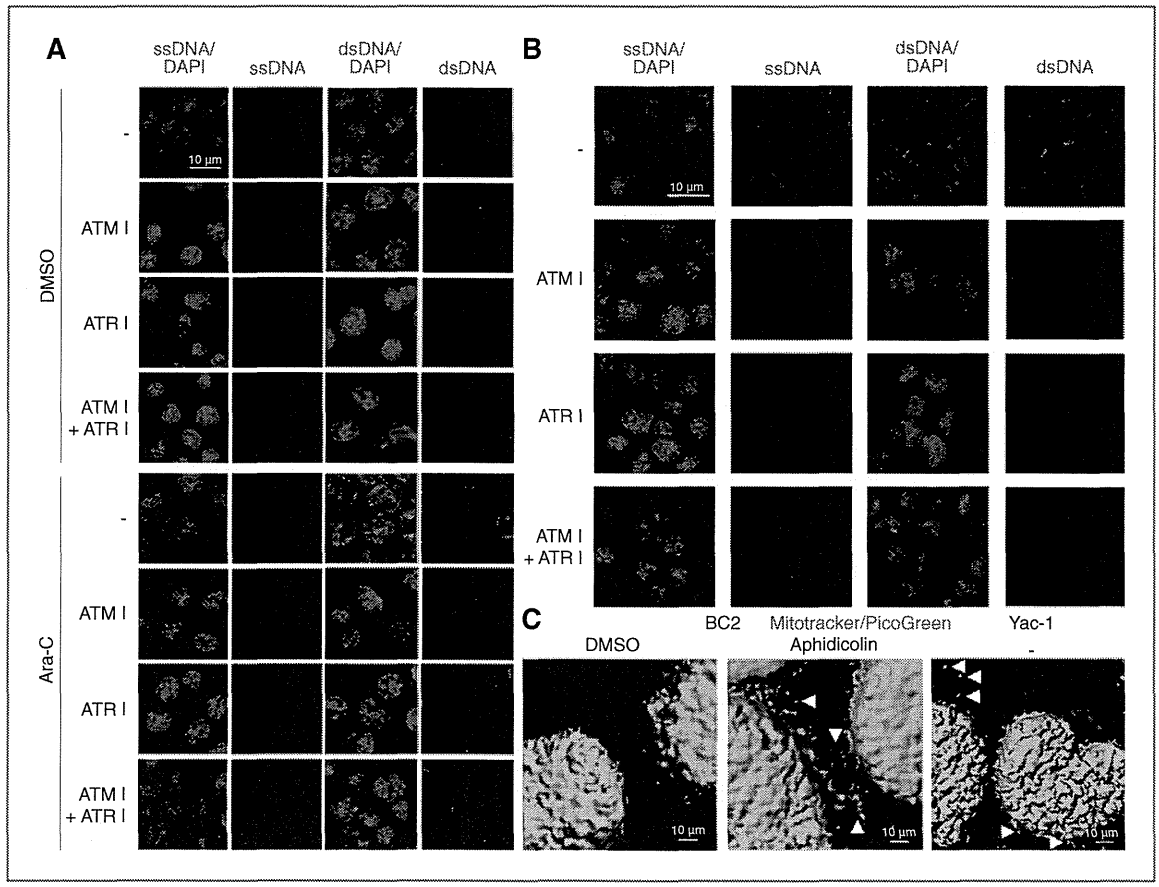

Figure 5. DNA damage leads to the appearance of cytosolic DNA. A, staining of BC2 cells for the presence of ssDNA (left columns) or dsDNA (right columns) in the presence of DAPI (first and third column). BC2 cells were pretreated with 10 μmol/L of the ATM inhibitor KU55933, the ATR inhibitor VE-821, KU55933+VE-821, or DMSO followed by treatment with DMSO or 10 μmol/L Ara-C for 14 hours. BC2 cells were treated with RNase and stained with ssDNA- or dsDNA-specific antibodies (red) and DAPI (blue). B, Yac-1 cells were treated with 10 μmol/L KU55933, VE-821, KU55933+VE-821, or DMSO for 14 hours and stained as outlined in A. C, DMSO (left) or 4 μmol/L aphidicolin-treated (middle; 14 hours) BC2 cells and Yac-1 cells (right) were incubated with the dsDNA-specific dye PicoGreen (green) for 1 hour and MitoTracker dye (red) for 15 minutes. Z-stack images were acquired by confocal microscopy and analyzed using Imaris software to generate iso-surface plots. White arrows, presence of cytosolic DNA.

inhibitor of nuclear DNA synthesis that activates the DDR but does not affect replication of mitochondrial DNA (Fig. 5C; Supplementary Fig. S4D; ref. 29). Three-dimensional rendering of confocal microscopy data showed that most cytosolic DNA is present outside of mitochondria in Yac-1 and Ara-C–treated BC2 cells (Fig. 5C; Supplementary Figs. S4D and S5).

To test whether the DDR influences the occurrence of cytosolic DNA, we pretreated BC2 cells with ATM and/or ATR inhibitors before treatment with Ara-C. Blocking of ATM and ATR prevented appearance of cytosolic DNA in response to Ara-C (Fig. 5A; Supplementary Fig. S6A). Strikingly, cytosolic DNA present in Yac-1 cells disappeared after inhibition of ATR for 14 hours (Fig. 5B; Supplementary Fig. S6B). Inhibition of ATM had a less pronounced effect on the occurrence of cytosolic DNA in agreement with effects observed on RAE1 expression and phosphorylation of IRF3 and TBK1 (Fig. 5A and B). However, the disappearance of cytosolic DNA in response to inhibition of ATM and ATR did not abrogate RAE1 expression in Yac-1 cells, suggesting that RAE1 expression is regulated by additional pathways (25). In summary, our data suggest that appearance of cytosolic DNA depends on the DDR and is rapidly turned over.

Cytosolic DNA induces RAE1 expression

To test whether cytosolic DNA induces RAE1 expression in BC2 cells, we transfected cells with Alexa-488–labeled plasmid DNA, genomic DNA, or ssDNA. We were unable to purify sufficient quantities of cytosolic DNA to determine whether cytosolic DNA present in Ara-C–treated BC2 cells directly induces RAE1 expression. Alexa-488–positive BC2 cells upregulated expression of RAE1, although to a lesser degree than Ara-C–treated cells (Fig. 6A).

The presence of DNA in the cytosol activates STING-dependent DNA sensors, leading to the activation of TBK1 and

Published OnlineFirst March 3, 2014; DOI: 10.1158/0008-5472.CAN-13-1703

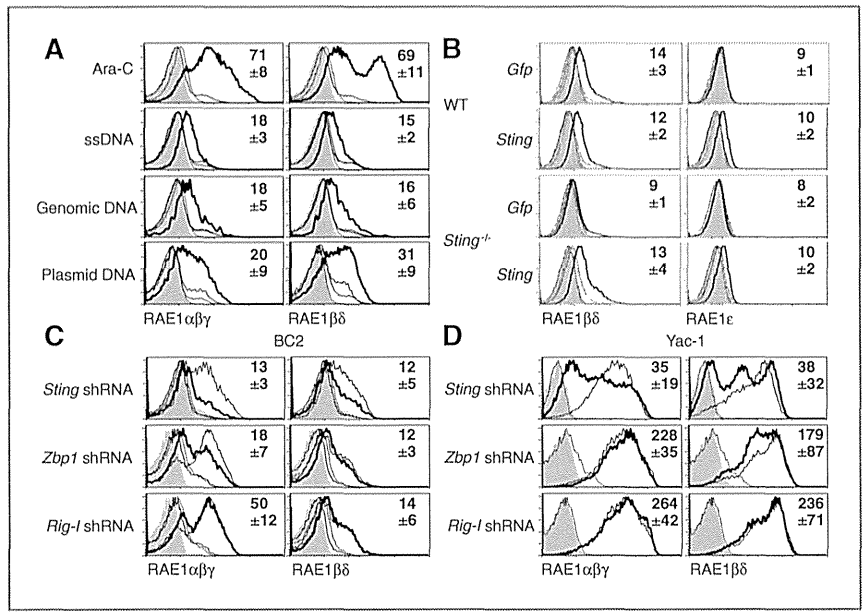

Figure 6. RAE1 expression is induced by cytosolic DNA and depends on STING. A, BC2 cells were transfected with 4 μg Alexa-488-labeled MSCV-IRES-*Gfp* plasmid DNA, C57BL/6 genomic DNA, or ssDNA. Some cells were treated with 10 μmol/L Ara-C or DMSO. Sixteen hours later, BC2 cells were stained for indicated NKG2DLs and analyzed by flow cytometry. Bold line, Ara-C–treated or Alexa-488$^+$ cells; dashed line, Alexa-488$^-$ or DMSO-treated cells; fine line, isotype staining of Ara-C–treated or Alexa-488$^+$ cells; dotted line, isotype staining of Alexa-488$^-$ cells; filled histograms, isotype staining of DMSO-treated cells. B, MEFs expressing nonfunctional or WT *Sting* were transduced with retroviral vectors encoding *Sting* or empty vector. Eight days after selection, cells were treated with 10 μmol/L Ara-C for 16 hours (bold line) or DMSO (fine line) and stained for indicated NKG2DLs. Isotype stainings of DMSO (filled histogram) or Ara-C–treated cells (dashed line) are shown. C, *Sting*-, *Zbp1/Dai*- and *Rig-I*–specific (bold line) or control shRNAs-transduced (fine line) BC2 cells were treated with 10 μmol/L Ara-C for 16 hours. Gene-specific (dashed line) or control shRNA-transduced (dotted line) BC2 cells were also treated with DMSO for 16 hours. NKG2DL expression was analyzed by flow cytometry. Filled histograms, isotype staining of Ara-C–treated cells. D, *Sting*-, *Zbp1/Dai*-, and *Rig-I*–specific (bold lines) or control shRNA-transduced (fine line) Yac-1 cells were stained for NKG2DL expression. Isotype staining of gene-specific (dashed line) or control shRNA (filled histogram)-transduced Yac-1 cells is shown. MFI ± SD are indicated.

IRF3 (8). We therefore tested whether STING is necessary for RAE1 expression in cells exposed to genotoxic stress. MEFs harboring a loss-of-function *Sting* mutation failed to upregulate RAE1 in response to Ara-C (Fig. 6B). Reconstitution of *Sting* expression resulted in restored inducibility of RAE1 in the cells. Furthermore, RAE1 induction by Ara-C was impaired in BC2 cells expressing a *Sting*-specific shRNA (Fig. 6C) and *Sting* inhibition in Yac-1 cells resulted in reduced constitutive RAE1 expression (Fig. 6D).

Next, we tested the requirement in RAE1 induction for one candidate STING-dependent DNA sensor, ZBP/DAI, that activates IRF3 (8). Knockdown of *Zbp1/Dai* partly inhibited the upregulation of RAE1αβγ in response to Ara-C, but had little effect on RAE1βδ (Fig. 6C). In contrast, knockdown of *Zbp1/Dai* modestly inhibited RAE1βδ but not RAE1αβγ expression in Yac-1 cells (Fig. 6D). Inhibition of *Rig-I*, a RNA sensor that may indirectly mediate responses to cytosolic DNA, had no effect on RAE1 expression in BC2 or Yac-1 cells (Fig. 6C and D). Hence, DNA sensors other than ZBP1/DAI are likely to participate in inducing RAE1 expression in response to DNA damage, in line with other evidence suggesting the existence of DNA sensors that act redundantly (30). Taken together, these data suggest that cytosolic DNA sensor pathways regulate RAE1 expression in cells exposed to DNA damage.

IRF3 regulates RAE1 expression in B-cell lymphomas of Eμ-*Myc* mice

To address whether IRF3 regulates RAE1 expression in lymphomas, *Irf3*-deficient mice were bred to mice overexpressing c-*Myc* under the control of immunoglobulin heavy-chain enhancer region (Eμ), analogous to human Burkitt lymphoma (31). Spontaneous B220^{low} B-cell lymphomas develop by 15 to 20 weeks of age and the progression of lymphomas is accelerated in NKG2D$^{-/-}$;Eμ-*Myc* mice (4, 32). Tumor cells in Eμ-*Myc* mice express phosphorylated ATM (ATMpS1981; Fig. 7A; ref. 19). Staining of tumor cells with a dsDNA-specific antibody revealed the presence of cytosolic dsDNA in B220^{low} tumor cells, but not normal B220$^+$ B cells (Fig. 7B). The accumulation of cytosolic DNA was strictly dependent on the DDR as administration of the ATM inhibitor KU55933 resulted in reduced levels of cytosolic dsDNA (Fig. 7C). *Irf3*$^{+/-}$;Eμ-*Myc* mice (median survival = 62 days) experienced a significantly reduced survival rate compared with *Irf3*$^{+/+}$;Eμ-*Myc* mice (median survival = 116 days; Fig. 7D). We were not able to generate *Irf3*$^{-/-}$;Eμ-*Myc* mice because *Irf3*$^{+/-}$;Eμ-*Myc* mice failed to breed. Heterozygosity of *Irf3* in Eμ-*Myc* mice resulted in 2.5-fold decrease of IRF3 levels and reduced expression of IRF3 target genes in splenic B-cell lymphomas when compared with *Irf3*$^{+/+}$;Eμ-*Myc* mice, suggesting that cytosolic DNA in

Published OnlineFirst March 3, 2014; DOI: 10.1158/0008-5472.CAN-13-1703

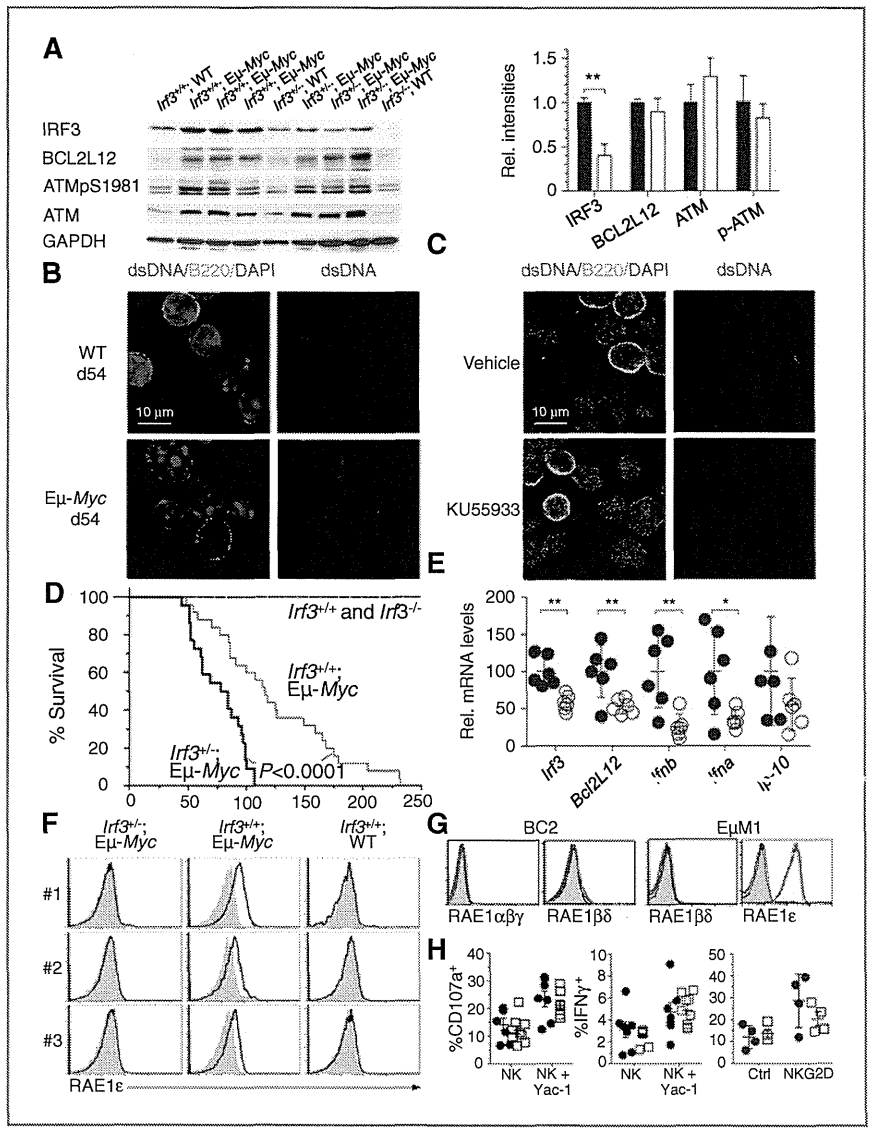

Figure 7. RAE1 expression in c-*Myc*-driven lymphomas depends on IRF3. A, immunoblot analysis of splenic B-cell lymphomas (>78% purity) from *Irf3*$^{+/-}$;Eμ-*Myc*, *Irf3*$^{+/+}$;Eμ-*Myc*, *Irf3*$^{+/+}$;WT, *Irf3*$^{+/-}$;WT, and *Irf3*$^{-/-}$;WT probed with antibodies for IRF3, BCL2L12, ATM, ATMpS1981, and GAPDH (left). Densitometry analysis of immunoblots showing mean ±SD from three mice normalized to GAPDH levels; **, $P < 0.01$. B, B220^{+} (green) cells of WT and Eμ-*Myc* mice were stained for dsDNA (red) in the presence of DAPI (blue) at 54 days of age. C, Eμ-*Myc* mice were injected intraperitoneally with 5 mg/kg KU55933 ($n = 3$) or vehicle ($n = 3$) at 34 and 36 days of age and stained for dsDNA (red), B220 (green), and DAPI (blue) at 38 days of age. D, *Irf3*$^{+/-}$;Eμ-*Myc* mice (thick) exhibit decreased survival compared with *Irf3*$^{+/+}$;Eμ-*Myc* (thin line), nontransgenic (dashed line), or *Irf3*$^{-/-}$ (dotted line) mice. The Kaplan–Meier analysis of survival of *Irf3*$^{+/+}$;Eμ-*Myc* mice ($n = 25$; median survival, 116 days), *Irf3*$^{+/-}$;Eμ-*Myc* mice ($n = 17$; median survival, 62 days), and *Irf3*$^{+/+}$ or *Irf3*$^{-/-}$ mice ($n = 25$; median survival, >250 days). $P < 0.0001$ by log-rank test or by the Gehan–Breslow–Wilcoxon test. E, relative mRNA levels of indicated IRF3 target genes in purified tumor cells of *Irf3*$^{+/-}$;Eμ-*myc* and *Irf3*$^{+/+}$;Eμ-*Myc* mice were measured by qRT-PCR. F, RAE1ε expression in tumor cells of three *Irf3*$^{+/-}$;Eμ-*Myc* mice. B220^{low} cells in blood of moribund *Irf3*$^{+/-}$;Eμ-*Myc*, *Irf3*$^{+/+}$;Eμ-*Myc*, and C57BL/6 mice (bold line) were stained for the indicated NKG2D ligand expression. Filled histogram, isotype staining of B220^{low} tumors. G, *Bcl2l12*-IRES-*Gfp* (red line) or IRES-*Gfp*–transduced (blue line) BC2 (left) or EμM1 (right) cells were stained for the indicated NKG2DLs 3 days posttransduction. Dashed line, isotype staining of *Bcl2l12*-IRES-*Gfp*–transduced cells. Fine line, isotype staining of IRES-*Gfp*–transduced cells. Filled histograms, isotype staining of untransduced cells. H, IL-2–activated NK cells derived from *Irf3*$^{+/-}$;Eμ-*Myc* (white squares, $n = 8$) or *Irf3*$^{+/+}$;Eμ-*Myc* (black circles, $n = 7$) mice were cocultured with Yac-1 cells at an effector to target ratio of 3:1. After 4 hours, the percentage of CD107a and IFN-γ–expressing NK1.1^{+}CD3^{-} cells was determined by flow cytometry (left and middle). Freshly isolated splenocytes of *Irf3*$^{+/-}$;Eμ-*Myc* (white squares, $n = 4$) and *Irf3*$^{+/+}$;Eμ-*Myc* (black circles, $n = 4$) mice were stimulated *in vitro* for 5 hours on plates coated with NKG2D-specific antibodies (MI-6, 10 μg/mL) or isotype control (10 μg/mL) before staining and analysis. Intracellular IFN-γ was detected by flow cytometry gated on NK1.1^{+}CD3^{-} cells (right). Error bar denotes SE of mean.

Published OnlineFirst March 3, 2014; DOI: 10.1158/0008-5472.CAN-13-1703

lymphomas activates IRF3 (Fig. 7A and E). Importantly, reduced levels of IRF3 in lymphomas impaired RAE1ε expression, the only RAE1 family member detected in Eμ-*Myc* tumor cells (Fig. 7F; ref. 33).

The null mutation introduced into the *Irf3* allele also resulted in functional inactivation of the neighboring *Bcl2l12* gene, which promotes or suppresses tumorigenesis depending on the cellular context (34, 35). However, heterozygosity of the gene-targeted locus did not result in reduced BCL2L12 levels or changes in the rate of apoptosis or proliferation of lymphomas (Supplementary Figs. S7A and S7B; Fig. 7A). Overexpression of *Bcl2l12* in BC2 and EμM1 cells, two cell lines derived from Eμ-*Myc* mice, had no effect on RAE1 expression, proliferation, or apoptosis (Fig. 7G; Supplementary Figs. S7C and S7D). We previously found that NK cells and T cells contribute to immunosurveillance in Eμ-*Myc* mice (18). However, *Irf3* deficiency had no impact on NK- and T-cell numbers or NK cell activity (Fig. 7H; ref. 36). In summary, our data suggest that RAE1 ligands are regulated by IRF3 in lymphomas of Eμ-*Myc* mice. Interestingly, IRF3 is likely to have additional functions in immunosurveillance as NKG2D deficiency increases the tumor load of Eμ-*Myc* mice, but has no impact on survival (4).

Discussion

Our previous results provided evidence that the DDR activates immune responses by inducing NKG2DLs (6). Here, we show that cytosolic DNA contributes to the induction of RAE1 expression in lymphoma cells in response to DNA damage for the following reasons: (i) inhibition of the DDR impaired the induction of cytosolic DNA and RAE1 molecules; (ii) transfection of DNA into cells upregulated RAE1 expression; (iii) inhibition of STING, TBK1, or IRF3 impaired RAE1 expression; (iv) TBK1 and IRF3 were activated in response to DNA damage in a DDR-dependent manner; and (v) overexpression of TBK1 or IKKε induced RAE1 expression.

Linking the DDR to STING-initiated pathways is of interest immunologically, because STING is a critical component of a major pathway common to receptors that detect cytosolic DNA and RNA of pathogens (8). Previous studies provided indications that the DDR induces phosphorylation of IRF3 and that certain Toll-like receptor agonists induce *Raet1* gene expression in peritoneal macrophages (37), but the linkage of these pathways had not been explored. Much remains to be determined about the relation of the DDR and STING pathways. We observed less phosphorylation of IRF3 in response to DNA damage when compared with LPS, suggesting that IRF3 translocation and transcriptional activity is differentially regulated in response to DNA damage. Consistent with this possibility, Noyce and colleagues reported that no minimal posttranslational modification of IRF3 correlated with its transcriptional activity (38). Of interest was that DNA damage consistently led to lower induction of IFN than Poly I:C. The reduced induction likely reflects the fact that the DDR failed to induce IRF7 activation, which is necessary for efficient transcription of IFN genes (data not shown).

Cytosolic DNA has been shown to be present in cells upon infection or the uptake of apoptotic cells (8). Our data show the presence of cytosolic DNA in uninfected lymphoma cell lines. An intriguing question is where cytosolic DNA originates from and the mechanism leading to cytosolic DNA in tumor cells. DNA damage is known to induce transcription of retroelements, including transposases, derived from functional endogenous retrovirus present in the genome (39). Alternatively, cytosolic DNA could be generated during DDR-dependent DNA repair that can result in deletion of genomic DNA.

An important question is the nature of the DNA sensor recognizing the cytosolic DNA. The induction of RAE1 by Ara-C partially relied on ZBP1/DAI. ZBP1/DAI is a candidate sensor that is reported to activate TBK1/IRF3 (40). However, additional TBK1-activating DNA sensors exist as MEFs from $Zbp1^{-/-}$-deficient mice mount a normal type I IFN response to DNA (18, 30). These sensors may be required for constitutive RAE1 expression in Yac-1 cells. Hence, unidentified DNA sensors may play a predominant role in YAC-1 cells, or may function redundantly with ZBP1/DAI, in the induction of RAE1.

NKG2D plays an important role in immunosurveillance of tumors in Eμ-*Myc* mice (4, 5). The accelerated development of lymphoma in *Irf3/Bcl2l12*$^{+/-}$;Eμ-*Myc* mice when compared with NKG2D-deficient mice suggests that IRF3 induces the expression of molecules other than RAE1 ligands important for immunosurveillance or suppression of tumorigenesis. IRF3 and BCL2L12 are known to induce genes implicated in apoptosis (11). However, we observed no differences in the rates of apoptosis or proliferation comparing WT and heterozygous tumor cells, suggesting that accelerated tumorigenesis of *Irf3/Bcl2l12*$^{+/-}$;Eμ-*Myc* mice is not due to effects of IRF3 or BCL2L12 on apoptosis or proliferation. In summary, our data suggest that tumorigenesis leads to accumulation of cytosolic DNA and subsequent activation of an antitumor immune response that may partially depend on NKG2D.

Disclosure of Potential Conflicts of Interest

No potential conflicts of interest were disclosed.

Authors' Contributions

Conception and design: A.R. Lam, N.L. Bert, D.H. Raulet, S. Gasser
Development of methodology: A.R. Lam, N. Le Bert, S.S. Ho, Y.J. Shen, C.X. Koo, S. Gasser
Acquisition of data (provided animals, acquired and managed patients, provided facilities, etc.): A.R. Lam, N. Le Bert, S.S. Ho, Y.J. Shen, M.L.F. Tang, G.M. Xiong, J.L. Croxford, C.X. Koo, K.J. Ishii, S. Gasser
Analysis and interpretation of data (e.g., statistical analysis, biostatistics, computational analysis): A.R. Lam, N. Le Bert, S.S. Ho, Y.J. Shen, M.L.F. Tang, C.X. Koo, K.J. Ishii, D.H. Raulet, S. Gasser
Writing, review, and/or revision of the manuscript: A.R. Lam, N. Le Bert, Y.J. Shen, D.H. Raulet, S. Gasser
Administrative, technical, or material support (i.e., reporting or organizing data, constructing databases): A.R. Lam, S. Akira
Study supervision: A.R. Lam, K.J. Ishii, S. Gasser

Grant Support

This work was supported by Biomedical Research Council grant 07/1/21/19/513, National Research Foundation grant HUJ-CREATE-Cellular and Molecular Mechanisms of Inflammation, and by grants from the US NIH to D.H. Raulet.

The costs of publication of this article were defrayed in part by the payment of page charges. This article must therefore be hereby marked *advertisement* in accordance with 18 U.S.C. Section 1734 solely to indicate this fact.

Received June 18, 2013; revised January 14, 2014; accepted February 1, 2014; published OnlineFirst March 3, 2014.

Published OnlineFirst March 3, 2014; DOI: 10.1158/0008-5472.CAN-13-1703

References

1. Raulet D. Roles of the NKG2D immunoreceptor and its ligands. Nat Rev Immunol 2003;3:781–90.
2. Gasser S, Raulet D. The DNA damage response, immunity and cancer. Semin Cancer Biol 2006;16:344–7.
3. Gasser S, Raulet DH. The DNA damage response arouses the immune system. Cancer Res 2006;66:3959–62.
4. Guerra N, Tan Y, Joncker N, Choy A, Gallardo F, Xiong N, et al. NKG2D-deficient mice are defective in tumor surveillance in models of spontaneous malignancy. Immunity 2008;28:571–80.
5. Raulet DH, Guerra N. Oncogenic stress sensed by the immune system: role of natural killer cell receptors. Nat Rev Immunol 2009;9:568–80.
6. Gasser S, Orsulic S, Brown EJ, Raulet DH. The DNA damage pathway regulates innate immune system ligands of the NKG2D receptor. Nature 2005;436:1186–90.
7. Rakoff-Nahoum S, Medzhitov R. Toll-like receptors and cancer. Nat Rev Cancer 2009;9:57–63.
8. Yanai H, Savitsky D, Tamura T, Taniguchi T. Regulation of the cytosolic DNA-sensing system in innate immunity: a current view. Curr Opin Immunol 2009;21:17–22.
9. Desmet CJ, Ishii KJ. Nucleic acid sensing at the interface between innate and adaptive immunity in vaccination. Nat Rev Immunol 2012;12:479–91.
10. Fitzgerald KA, McWhirter SM, Faia KL, Rowe DC, Latz E, Golenbock DT, et al. IKKepsilon and TBK1 are essential components of the IRF3 signaling pathway. Nat Immunol 2003;4:491–6.
11. Taniguchi T, Ogasawara K, Takaoka A, Tanaka N. IRF family of transcription factors as regulators of host defense. Annu Rev Immunol 2001;19:623–55.
12. Packham G, Cleveland JL. c-Myc and apoptosis. Biochim Biophys Acta 1995;1242:11–28.
13. Reimann M, Loddenkemper C, Rudolph C, Schildhauer I, Teichmann B, Stein H, et al. The Myc-evoked DNA damage response accounts for treatment resistance in primary lymphomas in vivo. Blood 2007;110:2996–3004.
14. Wang J, Boxer LM. Regulatory elements in the immunoglobulin heavy chain gene 3′-enhancers induce c-myc deregulation and lymphomagenesis in murine B cells. J Biol Chem 2005;280:12766–73.
15. Adams JM, Harris AW, Pinkert CA, Corcoran LM, Alexander WS, Cory S, et al. The c-myc oncogene driven by immunoglobulin enhancers induces lymphoid malignancy in transgenic mice. Nature 1985;318:533–8.
16. Corcoran LM, Tawfilis S, Barlow LJ. Generation of B lymphoma cell lines from knockout mice by transformation in vivo with an Emu-myc transgene. J Immunol Methods 1999;228:131–8.
17. Diefenbach A, Hsia JK, Hsiung MY, Raulet D. A novel ligand for the NKG2D receptor activates NK cells and macrophages and induces tumor immunity. Eur J Immunol 2003;33:381–91.
18. Croxford JL, Tang ML, Pan MF, Huang CW, Kamran N, Phua CM, et al. ATM-dependent spontaneous regression of early Emu-myc-induced murine B-cell leukemia depends on natural killer and T cells. Blood 2013;121:2512–21.
19. Sauer M, Reiners KS, Hansen HP, Engert A, Gasser S, von Strandmann EP. Induction of the DNA damage response by IAP inhibition triggers natural immunity via upregulation of NKG2D ligands in Hodgkin lymphoma in vitro. Biol Chem 2013;394:1325–31.
20. Kim ST, Lim DS, Canman CE, Kastan MB. Substrate specificities and identification of putative substrates of ATM kinase family members. J Biol Chem 1999;274:37538–43.
21. Servant MJ, Grandvaux N, Hiscott J. Multiple signaling pathways leading to the activation of interferon regulatory factor 3. Biochem Pharmacol 2002;64:985–92.
22. Hiscott J, Grandvaux N, Sharma S, Tenoever BR, Servant MJ, Lin R. Convergence of the NF-kappaB and interferon signaling pathways in the regulation of antiviral defense and apoptosis. Ann N Y Acad Sci 2003;1010:237–48.
23. Stein SC, Falck-Pedersen E. Sensing adenovirus infection: activation of interferon regulatory factor 3 in RAW 264.7 cells. J Virol 2012;86:4527–37.
24. Bartkova J, Horejsi Z, Koed K, Kramer A, Tort F, Zieger K, et al. DNA damage response as a candidate anti-cancer barrier in early human tumorigenesis. Nature 2005;434:864–70.
25. Raulet DH, Gasser S, Gowen BG, Deng W, Jung H. Regulation of ligands for the NKG2D activating receptor. Annu Rev Immunol 2013;31:413–41.
26. Fensterl V, Grotheer D, Berk I, Schlemminger S, Vallbracht A, Dotzauer A. Hepatitis A virus suppresses RIG-I-mediated IRF-3 activation to block induction of beta interferon. J Virol 2005;79:10968–77.
27. D'Incalci M, Covey JM, Zaharko DS, Kohn KW. DNA alkali-labile sites induced by incorporation of 5-aza-2′-deoxycytidine into DNA of mouse leukemia L1210 cells. Cancer Res 1985;45:3197–202.
28. Sancar A, Lindsey-Boltz LA, Unsal-Kaccmaz K, Linn S. Molecular mechanisms of mammalian DNA repair and the DNA damage checkpoints. Annu Rev Biochem 2004;73:39–85.
29. Zimmermann W, Chen SM, Bolden A, Weissbach A. Mitochondrial DNA replication does not involve DNA polymerase alpha. J Biol Chem 1980;255:11847–52.
30. Ishii KJ, Kawagoe T, Koyama S, Matsui K, Kumar H, Kawai T, et al. TANK-binding kinase-1 delineates innate and adaptive immune responses to DNA vaccines. Nature 2008;451:725–9.
31. Adams JM, Gerondakis S, Webb E, Corcoran LM, Cory S. Cellular myc oncogene is altered by chromosome translocation to an immunoglobulin locus in murine plasmacytomas and is rearranged similarly in human Burkitt lymphomas. Proc Natl Acad Sci U S A 1983;80:1982–6.
32. Harris AW, Pinkert CA, Crawford M, Langdon WY, Brinster RL, Adams JM. The E mu-myc transgenic mouse. A model for high-incidence spontaneous lymphoma and leukemia of early B cells. J Exp Med 1988;167:353–71.
33. Unni AM, Bondar T, Medzhitov R. Intrinsic sensor of oncogenic transformation induces a signal for innate immunosurveillance. Proc Natl Acad Sci U S A 2008;105:1686–91.
34. Nakajima A, Nishimura K, Nakaima Y, Oh T, Noguchi S, Taniguchi T, et al. Cell type-dependent proapoptotic role of Bcl2L12 revealed by a mutation concomitant with the disruption of the juxtaposed Irf3 gene. Proc Natl Acad Sci U S A 2009;106:12448–52.
35. Stegh AH, Kim H, Bachoo RM, Forloney KL, Zhang J, Schulze H, et al. Bcl2L12 inhibits post-mitochondrial apoptosis signaling in glioblastoma. Genes Dev 2007;21:98–111.
36. Sato M, Suemori H, Hata N, Asagiri M, Ogasawara K, Nakao K, et al. Distinct and essential roles of transcription factors IRF-3 and IRF-7 in response to viruses for IFN-alpha/beta gene induction. Immunity 2000;13:539–48.
37. Hamerman JA, Ogasawara K, Lanier LL. Cutting edge: Toll-like receptor signaling in macrophages induces ligands for the NKG2D receptor. J Immunol 2004;172:2001–5.
38. Noyce RS, Collins SE, Mossman KL. Differential modification of interferon regulatory factor 3 following virus particle entry. J Virol 2009;83:4013–22.
39. Wilkins AS. The enemy within: an epigenetic role of retrotransposons in cancer initiation. Bioessays 2010;32:856–65.
40. Takaoka A, Wang Z, Choi M, Yanai H, Negishi H, Ban T, et al. DAI (DLM-1/ZBP1) is a cytosolic DNA sensor and an activator of innate immune response. Nature 2007;448:501–5.